Journal of Controlled Release 385 (2025) 114041

Contents lists available at ScienceDirect

Journal of Controlled Release

journal homepage: www.elsevier.com/locate/jconrel

Repurposing mesalamine for acute kidney injury through supramolecular assembly

Byeongmin Park [a,b,1], Daeho Park [a,1], Hochung Jang [c,1], Yoon Sook Ko [d], Hee Young Lee [d], Young Eun Choi [d], Jiwoong Choi [a], Se Won Oh [d], Sang-Kyung Jo [d], Sun Hwa Kim [a,b], Yongju Kim [b,e], Sangmin Lee [f], Kwangmeyung Kim [g], Myung-Gyu Kim [d,**], Yoosoo Yang [c,**], Man Kyu Shim [a,h,*]

[a] Medicinal Materials Research Center, Biomedical Research Division, Korea Institute of Science and Technology (KIST), Seoul 02792, Republic of Korea
[b] KU-KIST Graduate School of Converging Science and Technology, Korea University, Seoul 02841, Republic of Korea
[c] Department of Integrative Biotechnology, Sungkyunkwan University, Suwon 16419, Republic of Korea
[d] Division of Nephrology, Department of Internal Medicine, Korea University Medical College, Seoul, 02841, Republic of Korea
[e] Chemical and Biological Integrative Research Center, Korea Institute of Science and Technology, Seoul 02792, Republic of Korea
[f] College of Pharmacy, Graduate School of Pharmaceutical Sciences, Kyung Hee University, Seoul 02453, Republic of Korea
[g] College of Pharmacy, Graduate School of Pharmaceutical Sciences, Ewha Womans University, Seoul 03760, Republic of Korea
[h] Division of Bio-Medical Science and Technology, KIST School, Korea University of Science and Technology, Seoul 02792, Republic of Korea

ARTICLE INFO

Keywords:
Acute kidney injury (AKI)
Drug repurposing
Mesalamine
Prodrug
Nanomedicine

ABSTRACT

Acute kidney injury (AKI) is a prevalent and life-threatening condition, particularly in patients undergoing high-risk surgeries, where the incidence can exceed 50 %. Despite its growing impact, therapeutic options remain limited, with dialysis being the primary treatment. Drug repurposing offers a better risk-versus-reward trade-off for accelerating the development of effective therapies. Mesalamine, a clinically approved anti-inflammatory agent for ulcerative colitis, can be a promising candidate for AKI treatment due to its ability to modulate various inflammatory pathways. However, their risk of nephrotoxicity from systemic exposure underscores the need for strategies to control off-target effects. Here, we propose a mesalamine prodrug, a conjugate between mesalamine and a cathepsin B-cleavable peptide, which spontaneously forms nanoassemblies through intermolecular interactions. In a mouse AKI model, these nanoassemblies accumulate in the inflamed kidney by becoming trapped between disrupted tight junctions, subsequently releasing mesalamine precisely at the site of injured tubular cells to alleviate the disease. Meanwhile, side effects from non-specific drug release are minimized as the nanoassemblies remain inactive in healthy tubular cells and other normal organs with relatively low cathepsin B expression. This study provides valuable insights into a rational approach to facilitating drug repositioning for the effective and safer use of mesalamine in AKI.

1. Introduction

Acute kidney injury (AKI) is a clinical syndrome characterized by a sudden decline in renal function, affecting approximately 21 % of hospitalized patients and contributing to high rates of morbidity and mortality [1]. Renal ischemia-reperfusion injury (IRI) is a major cause of AKI, particularly in patients undergoing high-risk surgeries such as cardiovascular procedures or in those with conditions like sepsis or hypovolemic shock, where the incidence can reach 50–80 % [2,3]. Renal IRI disrupts kidney microvascular integrity and activates inflammatory pathways, thereby exacerbating both local and systemic inflammatory responses [4,5]. Despite its increasing incidence and the significant healthcare burden it poses, therapeutic options for AKI are limited to dialysis, which is merely a symptomatic and palliative approach [6].

* Corresponding author at: Medicinal Materials Research Center, Biomedical Research Division, Korea Institute of Science and Technology (KIST), Seoul 02792, Republic of Korea.
** Corresponding authors.
E-mail addresses: gyu219@hanmail.net (M.-G. Kim), yangys@skku.edu (Y. Yang), mks@kist.re.kr (M.K. Shim).
[1] These authors contributed equally as co-first authors.

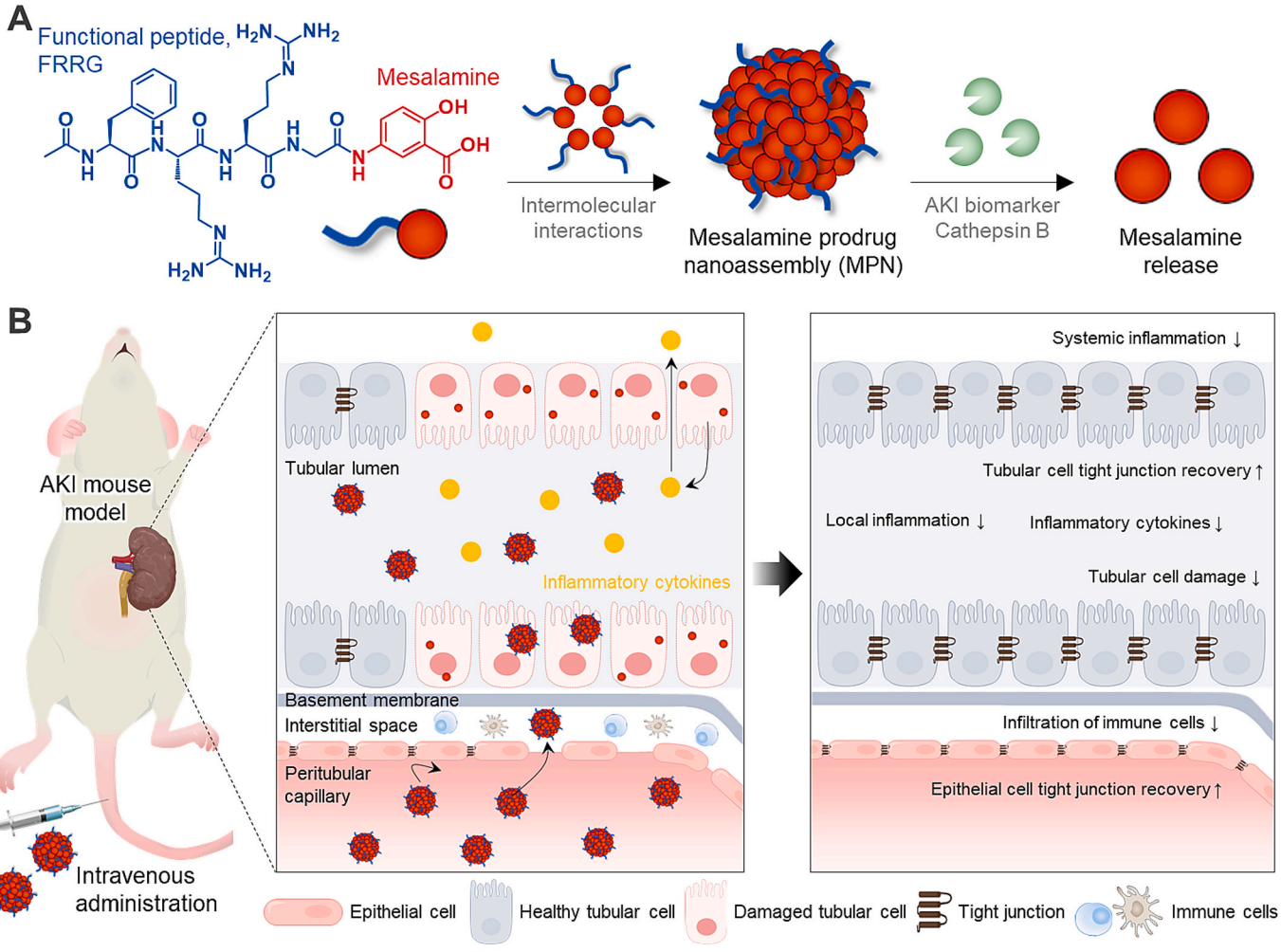
https://doi.org/10.1016/j.jconrel.2025.114041
Received 5 April 2025; Received in revised form 2 July 2025; Accepted 12 July 2025
Available online 17 July 2025
0168-3659/© 2025 The Authors. Published by Elsevier B.V. This is an open access article under the CC BY-NC license (http://creativecommons.org/licenses/by-nc/4.0/).

Given the urgent need for effective AKI treatments and the limitations of current options, drug repurposing—the identification of new therapeutic uses for existing drugs—offers several benefits, including reduced development time, lower costs and potentially more assured safety profiles, compared to de novo drug development [7,8]. Mesalamine (5-aminosalicylic acid), primarily used to treat mild to moderate ulcerative colitis, works by downregulating the production of pro-inflammatory cytokines and chemokines and inhibiting the mitogen-activated protein kinase (MAPK) pathway, which plays a key role in the inflammatory response [9,10]. Considering its long-standing clinical use alongside these extensive anti-inflammatory effects, mesalamine could be a promising candidate for repurposing as a new treatment option for AKI.

However, its application for kidney-related pathological conditions is hindered by significant concerns about nephrotoxicity [11]. A clinically well-known adverse effect of treatment with mesalamine in patients with inflammatory bowel disease (IBD) is interstitial nephritis, which can lead to progressive renal damage and chronic kidney disease [12]. This nephrotoxicity arises from mesalamine's extensive systemic exposure due to significant absorption in the upper gastrointestinal (GI) tract following oral administration [13]. High intrarenal concentrations of mesalamine may amplify oxidative damage and inflammation, further contributing to kidney injury [14]. Additionally, mesalamine has been associated with rare but severe adverse effects of myocarditis and pancreatitis, further limiting its use in vulnerable patient populations [15,16]. These considerations highlight the need for the development of methodologies to precisely control the activity of mesalamine at the target site for its repurposing to AKI.

We herein propose a promising approach to overcome these limitations through the effectively coordinated mesalamine prodrug nanoassembly (MPN) for the treatment of AKI (Scheme 1A). This formulation enhances target selectivity and reduces the side effects of mesalamine through linkage with a cathepsin B-specific cleavable peptide, FRRG (Phe-Arg-Arg-Gly). The key components include: i) an "F" residue that promotes self-assembly of the system by intermolecular π-π interactions between aromatic segments [17–21], ii) an "RR" motif cleavable by cathepsin B, which is overexpressed as a biomarker in injured tubular cells [22–25] and iii) a "G" spacer sequence to enhance the sensitivity toward target enzyme. Thus, these prodrugs spontaneously self-assemble in the aqueous phase without requiring additional carrier materials (e.g., polymers, lipids and other organic/inorganic substances), leading to significant advantages such as high drug loading capacity and minimized risk of potential toxicity related to these substances.

In an ischemia-reperfusion-induced AKI (IR-AKI) model, the MPNs administered intravenously accumulates passively in inflamed kidneys



Scheme 1. The methodology for repurposing mesalamine in acute kidney injury (AKI). This study aims to repurpose mesalamine, a clinically approved anti-inflammatory agent for ulcerative colitis, for the treatment of AKI. (A) Conjugation of the functional peptide FRRG enables the resulting mesalamine prodrugs to spontaneously form nanoparticles (MPNs) through intermolecular interaction-mediated supramolecular assembly. (B) In a mouse AKI model, MPNs accumulate in the inflamed kidney by becoming trapped between disrupted tight junctions, subsequently releasing mesalamine precisely at the site of injured tubular cells to alleviate the disease.

due to being trapped by disrupted tight junctions during the progression of the disease (Scheme 1B). Upon reaching the target site, the cathepsin B in injured tubular cells triggers the release of mesalamine, which alleviates inflammation by modulating the MAPK signaling pathways. In contrast, the nanoassemblies remain inactive in healthy tubular cells with relatively low cathepsin B expression, thus preventing the exacerbation of AKI due to unwanted drug exposure. In a similar context, treatment with MPNs also mitigates off-target toxicity to other healthy organs observed with the administration of mesalamine, highlighting its potential for targeted, effective and safe management of AKI patients. This study identifies both functional and structural improvements in AKI using animal and human samples, ultimately introducing a nanomedicine approach that efficiently targets these changes to repurpose mesalamine effectively.

2. Results and discussion

2.1. Synthesis and characterizations of MPNs

MPNs were prepared via the self-assembly of the mesalamine prodrugs in an aqueous solution. The mesalamine prodrug was synthesized through a one-step chemical conjugation of mesalamine and the FRRG peptide by amide condensation and characterized using an high-performance liquid chromatography (HPLC) system (Fig. S1). The MPNs exhibited an average size of 123.4 ± 11.48 nm and a spherical morphology with a uniform size distribution (Fig. 1A and B). A previous study identified the driving force for the self-assembly of the mesalamine prodrug into MPNs as hydrogen bonding and π-π stacking interactions between the mesalamine molecules and the aromatic rings of phenylalanine, respectively [26–28]. The nanoassemblies also demonstrated exceptional stability under serum conditions, maintaining their hydrodynamic size and polydispersity index (PDI) without significant changes for 48 h (Fig. 1C and S2). These highly stable nano-sized particles under blood conditions result in prolonged circulation in vivo, enhancing the likelihood of their accumulation in inflamed renal tissues due to capture by disrupted tight junctions.

The target biomarker-specific cleavage of MPNs was assessed after incubation with various enzymes. Rapid cleavage of approximately 99 % MPNs occurred within 1 h when exposed to cathepsin B, resulting in the release of mesalamine (Fig. 1D and S3). In contrast, no detectable cleavage was observed in the absence of cathepsin B after 24 h of incubation, showing that MPNs do not undergo non-specific hydrolysis. Comparable results were also noted when the nanoassemblies were incubated for 24 h with other enzymes, such as cathepsin D, E, L, caspase-3 (Cas-3) and matrix metalloproteinase-9 (MMP-9; Fig. S4). Finally, while treatment with mesalamine led to considerable cell death in the proximal tubular cell line HK-2, no significant toxicity was observed with MPN treatment at a high dose containing the same amount of mesalamine (Fig. 1E). This shows that non-inflamed, healthy tubular cells express an insufficient level of cathepsin B to induce the release of mesalamine from MPNs, ultimately suggesting that this may prevent the exacerbation of AKI caused by the toxic side effects of mesalamine.

The anti-inflammatory potential of MPNs was investigated HK-2 cells after treatment with hydrogen peroxide (H_2O_2) to mimic IR-AKI conditions. Immediately following reperfusion of ischemic renal tissue, cells generate large amounts of reactive oxygen species (ROS), including H_2O_2, superoxide anions and hydroxyl radicals. First, HK-2 cells upregulated cathepsin B to 2.3 to 2.41 times higher after incubation with H_2O_2 compared to the naive cells, indicating a significant overexpression of the target enzyme in injured hepatocytes (Fig. 1F). MPNs exerted anti-inflammatory effects in injured cells through the release of mesalamine via enzymatic cleavage by elevated cathepsin B, resulting in the modulation of pathways related to kidney inflammation. Excessive ROS causes cellular oxidative damage, which in turn upregulate the MAPK signaling pathway that play a crucial role in regulating kinases

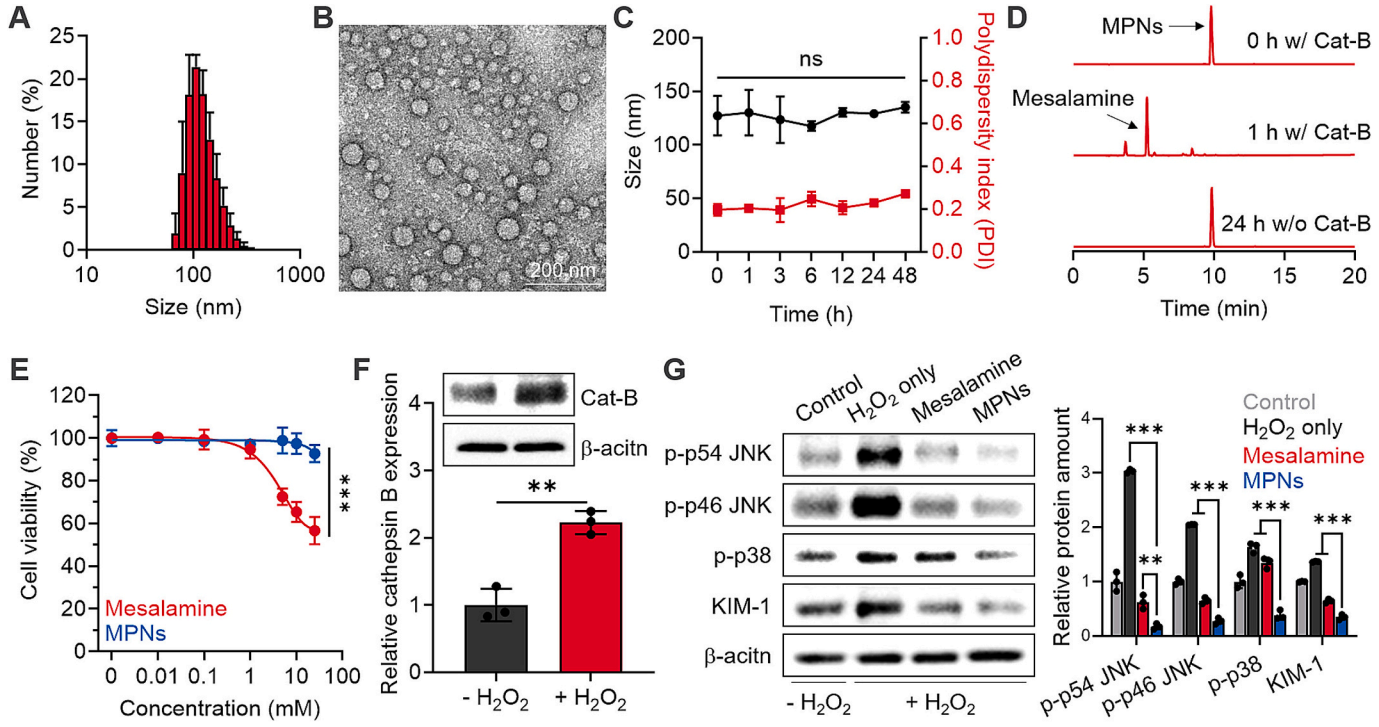


Fig. 1. Physicochemical characterization of MPNs. (A) Hydrodynamic size distribution and (B) TEM image of MPNs. (C) Changes in hydrodynamic size and polydispersity index (PDI) of MPNs in mouse serum over 48 h ($n = 3$). (D) Cleavage behavior of MPNs in the presence or absence of cathepsin B (Cat-B). (E) Cytotoxicity of mesalamine and MPNs toward tubular cells (n = 3). (F) Relative expression of cathepsin B in tubular cells before and after H_2O_2 treatment (n = 3). (G) Relative expression of MAPK and KIM-1 in H_2O_2-treated tubular cells and those incubated with mesalamine or MPNs (n = 3). Data are represented as mean ± SEM. $P^{ns} > 0.05$, $^{**}P < 0.01$, $^{***}P < 0.001$; significance was determined by one-way ANOVA with Tukey's post hoc test (B, F) or Student's *t*-test (D, E).

involved in kidney diseases [29]. Exposure of HK-2 cells to H_2O_2 induced a significant upregulation of MAPK family proteins, phosphorylated c-Jun N-terminal kinases (JNKs) and p38. Subsequent treatment with MPNs effectively decreased the levels of these inflammatory mediators, including p-p54 JNK, p-p46 JNK and p-p38, as well as the kidney injury marker KIM-1 (Fig. 1G). Importantly, the effects of MPNs in downregulating the MAPK signaling pathway were more pronounced than those of mesalamine, owing to the enhanced cellular uptake facilitated by nanoparticle formulation [30]. Taken together, these findings indicate that MPNs, composed solely of mesalamine prodrugs without any additional carrier materials, could potentially target inflamed kidneys, subsequently releasing mesalamine selectively at the cathepsin B-overexpressed injured tubular cells.

2.2. Enhanced renal accumulation of MPNs

Next, we aimed to investigate the in vivo availability and localization of MPNs in injured kidneys compared to normal kidneys under the pathological conditions of IR-AKI. As expected, significant upregulation of cathepsin B was observed in renal tissues from AKI patients and animal models (Fig. 2A and S5). Additionally, disruption of tight juntions was confirmed by demonstrating the loss of two major tight junction-associated proteins, occludin-1 and zonula occludens-1 (ZO-1), in both injured kidney samples compared to healthy tissues (Fig. 2B and S6). Nanoparticles larger than 100 nm in diameter generally cannot pass through the glomerular filtration barrier and eventually extreted via the renal tubule system [31]. However, we expected that inflamed kidneys would allow passive accumulation of nanoparticles due to the disruption of tight junctions between epithelial cells in the peritubular capillaries.

Interestingly, whole-body near-infrared fluorescence (NIRF) images of AKI mice revealed substantial accumulation of MPNs in the kidneys (highlighted by the red dotted line) compared to the Sham group (Fig. 2C). Ex vivo fluorescence images of major organs excised from AKI mice 6 h after MPN administration further showed significantly higher accumulation in the inflamed kidneys than healthy renal tissues (Fig. 2D). MPNs exhibited typical in vivo nanoparticle behavior, accumulating in the liver after entering the bloodstream due to several factors (e.g., large blood volume, slow sinusoidal blood flow and the presence of Kupffer cells), followed by renal excretion (Fig. S7) [32]. Histological analysis directly visualized the localization of MPNs within the inflamed tissues of AKI mice, demonstrating marked accumulation in both the renal medulla and cortex, the primary sites of lesions, compared to normal mice (Fig. 2E and S8). Further investigation showed that the nanoasseemblies were mostly cleared from the kidneys of normal mice by 24 h, whereas their persistent retention in the inflamed kidneys was observed even 48 h after injection (Fig. 2F). As a control, hyaluronic acid (HA) nanoparticles failed to accumulate within injured renal tissues due to their relatively larger size of 200 nm compared to MPNs (Fig. S9). Importantly, there were no differences in renal accumulation of HA nanoparticles between sham and AKI mice. These results verify that MPNs with appropriate physical features passively target inflamed renal tissues through disrupted tight junctions during the onset of AKI, leading to sustained retention over a long period.

2.3. Therapeutic efficacy of MPNs in IR-AKI Model

The in vivo anti-inflammatory effects of MPNs were assessed in an IR-AKI mouse model with four groups: (i) untreated healthy mice (Sham), (ii) IR-AKI + PBS (PBS), (iii) IR-AKI + mesalamine (mesalamine) and (iv) IR-AKI + MPNs (MPNs). The mice were intravenously injected with an equivalent dose of mesalamine or MPNs based on the active compound 1 h after the onset of of IR injury, followed by analysis 24 h after administration (Fig. 3A). MPN treatment led to a significant improvement in renal function deterioration compared to the PBS and mesalamine groups (Fig. 3B). The anti-inflammatory effects of the nanoassemblies were further evaluated by measuring inflammatory cytokines in kidney tissues. IR injury triggers the release of pro-inflammatory cytokines in the kidneys, which recruit activated white blood cells and ultimately exacerbate inflammation, cell damage and organ dysfunction [33]. The MPN group demonstrated a pronounced decrease in the levels of tumor necrosis factor alpha (TNF-α), interferon gamma (IFN-γ), interleukin-1 beta (IL-1β) and IL-6 compared to the PBS and mesalamine groups (Fig. 3C). In contrast, the anti-inflammatory cytokine, IL-10 returned to levels similar to those of the sham group following MPN treatment (Fig. 3D). A single 6 mg/kg dose of MPNs fully restored renal function impaired by IRI within 24 h to levels comparable to the sham group, whereas lower doses of 1 or 3 mg/kg resulted in minimal therapeutic effect (Fig. S10). In contrast, mesalamine failed to show any therapeutic effects compared to the PBS group, which can originates from the unfavorable pharmacokinetic (PK) profile of the small molecule structure that exhibits rapid in vivo clearance.

Pathological analysis revealed that kidney tissues treated with MPNs showed significantly alleviated renal congestion compared to those clearly observed in the PBS and mesalamine groups (Fig. 3E and S11). Histopathological analysis using periodic acid-schiff (PAS) staining also revealed reduced tubular damage and renal congestion in MPN-treated mice compared to those in the PBS and mesalamine groups (Fig. 3F). Additionally, MPN treatment reduced the infiltration of F4/80-positive macrophages and Ly6G-positive neutrophils in the injured renal tubulointerstitium (Fig. 3G). TUNEL staining also showed a decrease in apoptotic cells in kidney tissues from AKI mice treated with MPNs compared to those treated with PBS or mesalamine (Fig. 3H). Treatment with mesalamine resulted in significantly greater apoptotic cell death compared to the PBS group, indicating renal damage due to its cytotoxicity, as shown in Fig. 1D. These results suggest that MPNs minimize mesalamine-related nephrotoxicity through selective drug release in cathepsin B-overexpressing injured tubular cells, effectively restoring kidney structure and function without the risk of side effects.

To directly investigate the mechanism by which MPNs reduce mesalamine toxicity, we assessed their pharmacokinetic (PK) profile in an IR-AKI mouse model. Following intravenous administration, MPNs remained detectable in the blood for up to 24 h, indicating prolonged circulation in vivo (Fig. S12A). Additionally, no degradation occurred after 48 h of incubation in mouse serum (Fig. S12B). For the pharmacodynamic (PD) analysis of MPNs, we first evaluated cathepsin B levels in normal organs and the inflamed kidney, observing significantly higher expression in the injured renal tissue (Fig. S13A). Subsequent incubation of MPNs with lysates from each organ resulted in degradation into free mesalamine only in the inflamed kidney lysate (Fig. S13B). These findings suggest that MPNs remain highly stable in the bloodstream and off-target organs, without non-specific cleavage into mesalamine.

2.4. The restoration of renal barriers to prevent systemic inflammation by MPNs

We next investigated whether the anti-inflammatory effects of MPNs restore the disruption of tight junctions in inflamed kidneys, thereby suppressing systemic inflammation caused by the leakage of pro-inflammatory cytokines and immune cells through compromised renal barriers. In AKI mice, mesalamine had a slight effect on recovering the destruction of renal tight junctions, as evidenced by the slightly increased expression of ZO-1 and occludin-1 in the inflamed kidneys compared to the PBS group (Fig. 4A). Notably, renal tissues from AKI mice treated with MPNs showed significantly restored tight junctions, with ZO-1 and occludin-1 levels nearly comparable to those in the Sham group. This resulted in a marked decrease in the serum levels of TNF-α, IFN-γ, IL-1β and IL-6, whereas these levels remained similarly elevated in AKI mice treated with PBS or mesalamine (Fig. 4B). To further assess the impact of systemic inflammation due to cytokine leakage, we analyzed hematological parameters indicative of hepatic and cardiac toxicities, including aspartate aminotransferase (AST), alanine

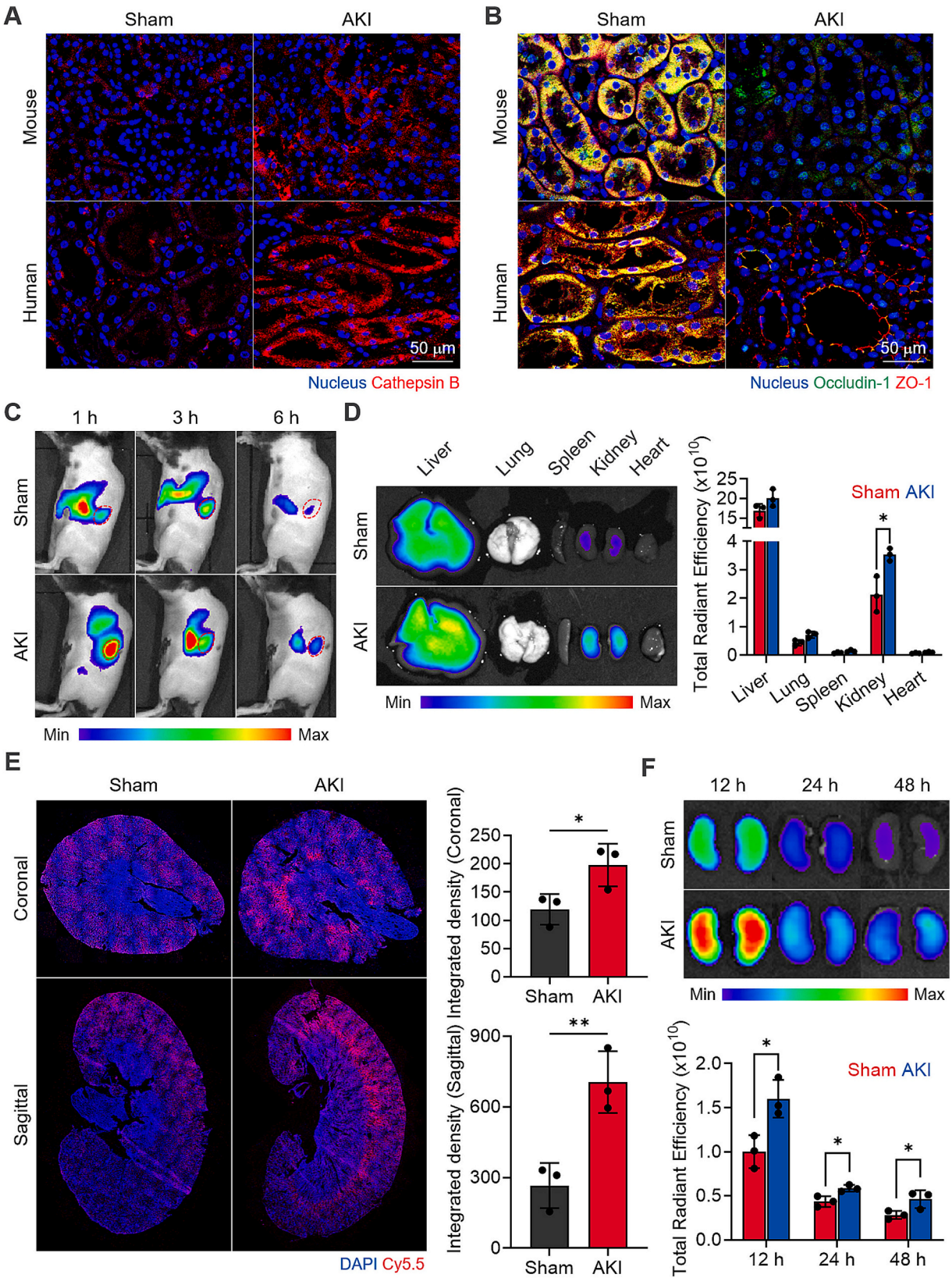


Fig. 2. Biomarker identification and selective accumulation of MPNs in injured kidneys. Expression of (A) cathepsin B and (B) tight junctions in renal tissues from healthy mice and humans or those with AKI. (C) Whole-body NIRF images of sham and AKI mice after intravenous administration of MPNs. (D) Ex vivo NIRF images 6 h post-treatment with MPNs (n = 3). (E) Representative confocal microscopy images of kidney tissues from sham and AKI mice treated with MPNs (n = 3). (F) Time-dependent renal accumulation of MPNs (n = 3). Data are represented as mean ± SEM. *$P < 0.05$, **$P < 0.01$; significance was determined by one-way ANOVA with Student's t-test (D, E, F).

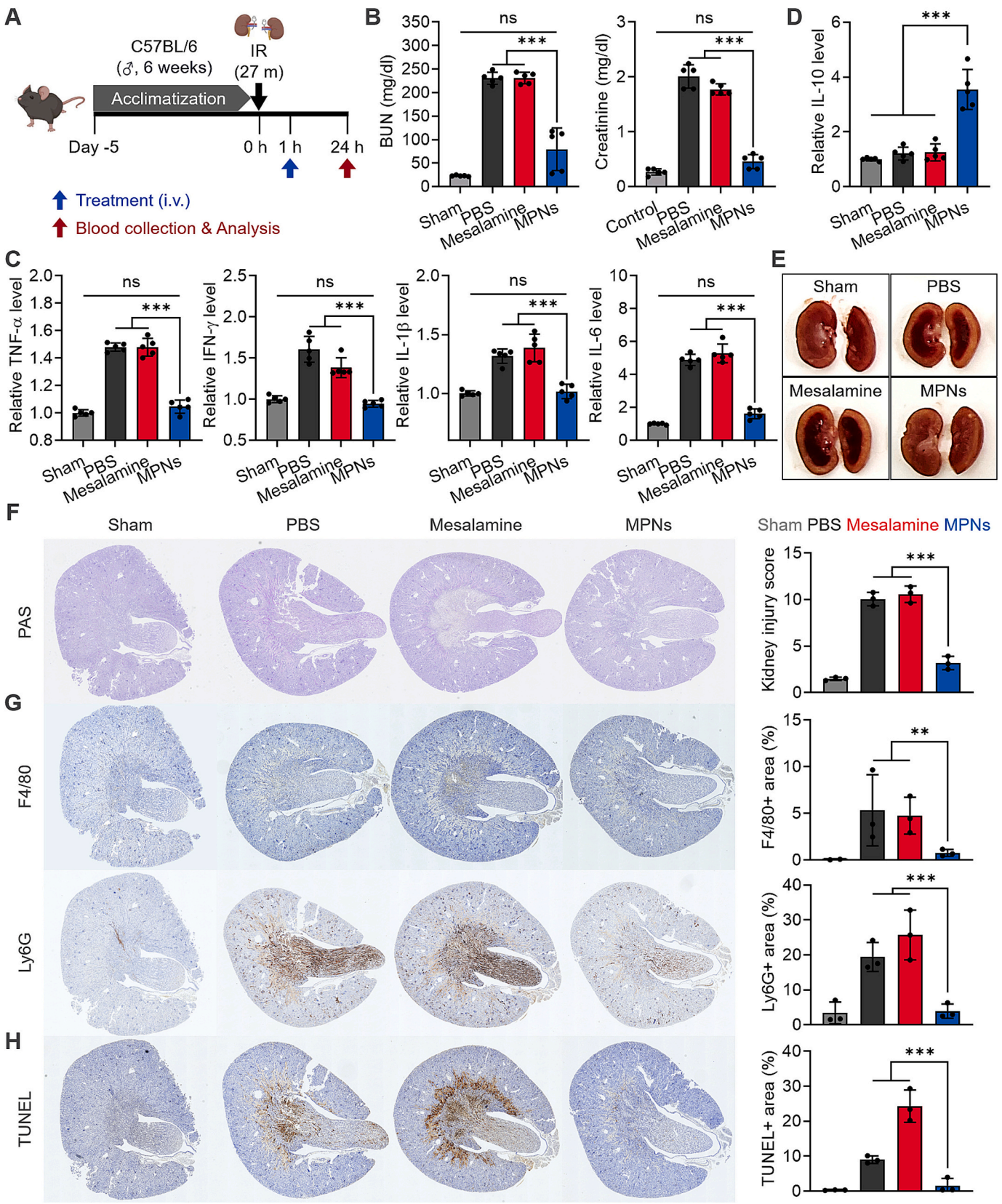


Fig. 3. Therapeutic efficacy of MPN treatment in the IR-AKI mouse model. (A) Treatment schedule. Mesalamine and MPN, with an equivalent active ingredient dose, were intravenously injected 1 h after IR injury. (B) Serum levels of BUN and creatinine in AKI mice after 24 h of treatment with mesalamine or MPNs ($n = 5$). Relative levels of (C) pro-inflammatory and (D) anti-inflammatory cytokines in kidneys (n = 5). (E) Representative optical images of renal tissues after 24 h of treatment with mesalamine or MPNs. Histology of kidney tissues stained with (F) PAS, (G) F4/80, Ly6G or (H) TUNEL (n = 3). Data are represented as mean ± SEM. ***$P < 0.001$; significance was determined by one-way ANOVA with Tukey's post hoc test.

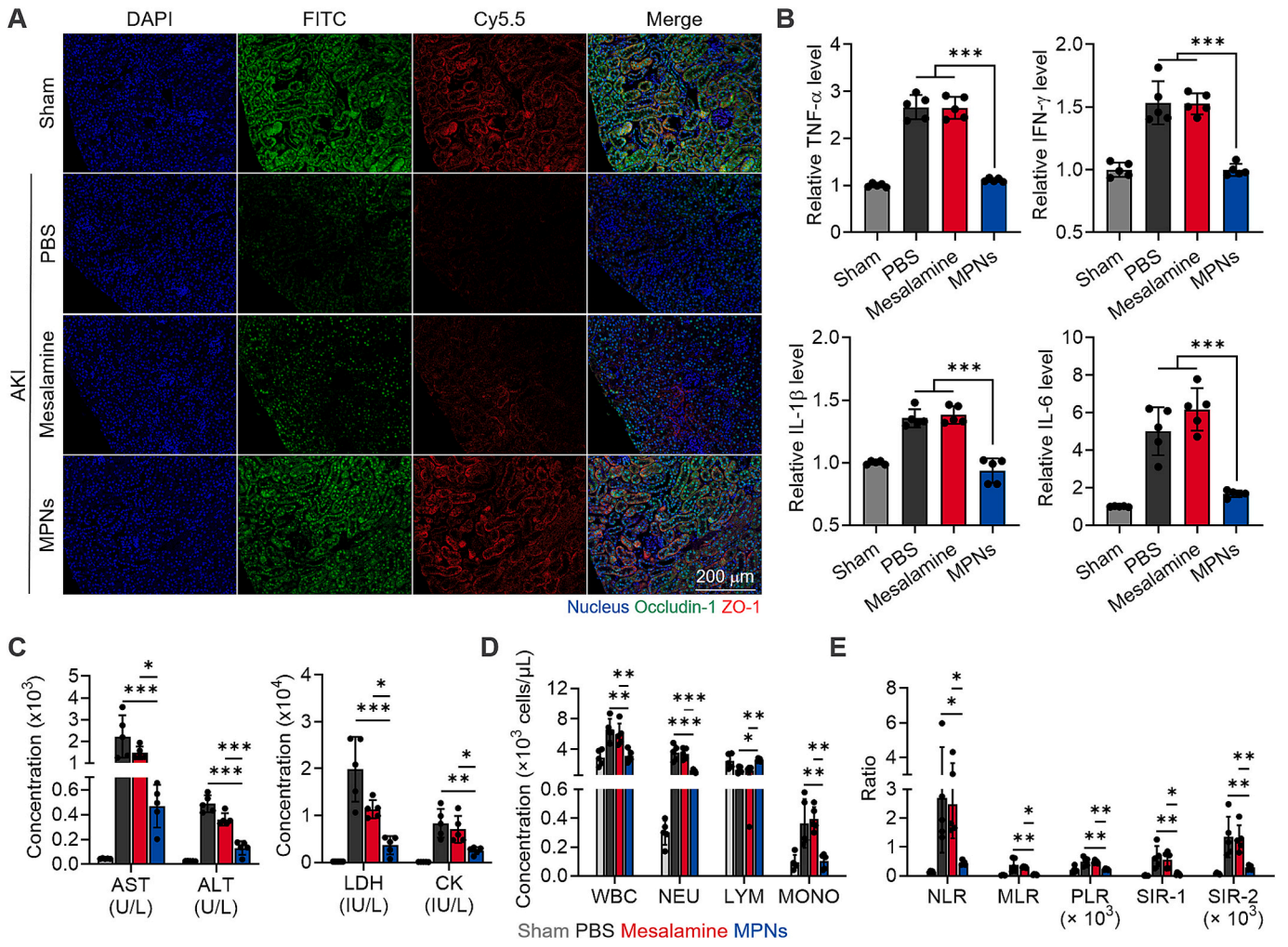


Fig. 4. Prevention of systemic inflammation through the restoration of tight junctions by MPNs. (A) Representative confocal microscopy images of renal tissues stained with anti-occludin-1 and anti-ZO-1 antibodies. (B) Serum levels of pro-inflammatory cytokines (n = 5). Hemanalysis results of (C) blood chemistry, (D) complete blood count (CBC) and (E) inflammatory hematological ratios (n = 5). Data are represented as mean ± SEM. $^{*}P < 0.05$, $^{**}P < 0.01$, $^{***}P < 0.001$; significance was determined by one-way ANOVA with Tukey's post hoc test.

transaminase (ALT), lactate dehydrogenase (LDH) and creatine kinase (CK), as well as white blood cell (WBC), neutrophil (NEU), lymphocyte (LYM) and monocyte (MONO) counts (Fig. 4C, D and S14). While both the PBS and mesalamine groups exhibited notable alterations in these parameters compared to the Sham group, AKI mice treated with MPNs showed substantial improvements, with some indicators returning to near-normal levels. In addition, MPN-treated AKI mice demonstrated better outcomes in systemic inflammation markers and histologic changes, including the neutrophil-to-lymphocyte ratio (NLR), monocyte-to-lymphocyte ratio (MLR), platelet-to-lymphocyte ratio (PLR), systemic inflammation response index (SIRI) and systemic immune inflammation index (Fig. 4E). Consistent with these findings, H&E staining of major organs revealed considerable structural abnormalities and injury in the PBS and mesalamine groups, but no such histological toxicity was observed in the MPN group (Fig. S15). Taken together, our findings highlight the exceptional ability of nanoassemblies to effectively suppress both local and systemic inflammation in AKI sites, demonstrating remarkable therapeutic potential.

2.5. *In vivo safety of MPNs*

The safety of MPN treatment was assessed in healthy C57BL/6 mice, which received single or multiple intravenous doses. The single-dose concentration was twice that used in the therapeutic efficacy study, while the multiple doses were administered daily three times at the same concentration as the therapeutic dose. No changes in body weight were observed after single or multiple doses of MPNs compared to the untreated control group (Fig. 5A). In contrast, both groups treated with mesalamine experienced significant body weight loss. Additionally, hematological parameters related to hepatic function (AST and ALT), renal function (BUN and creatinine) and cardiac function (LDH and CK) showed considerable increases in the mesalamine-treated group, whereas these levels in the MPN-treated group remained comparable to those in healthy mice (Fig. 5B). Interestingly, hematological toxicity was more pronounced in mice treated with a single dose of mesalamine compared to those receiving multiple doses. Similar results were also noted in histological analyses, where structural abnormalities in major organs were severe after mesalamine single dose than multiple dose (Fig. 5C). In contrast, no histopathological toxicity was observed in the MPN group. As a substantial amount of MPNs remained in the kidney 24 h after administration (Fig. S7), repeated dosing may lead to considerable renal accumulation. Nevertheless, no adverse effects related to body weight, hematology or histology were observed compared to mesalamine-treated mice, underscoring the excellent safety profile. These findings indicate that the nanoassemblies minimize the side effects of mesalamine while effectively suppressing both local and systemic inflammation, demonstrating their potential as a valuable medication for the effective and safe treatment of AKI.

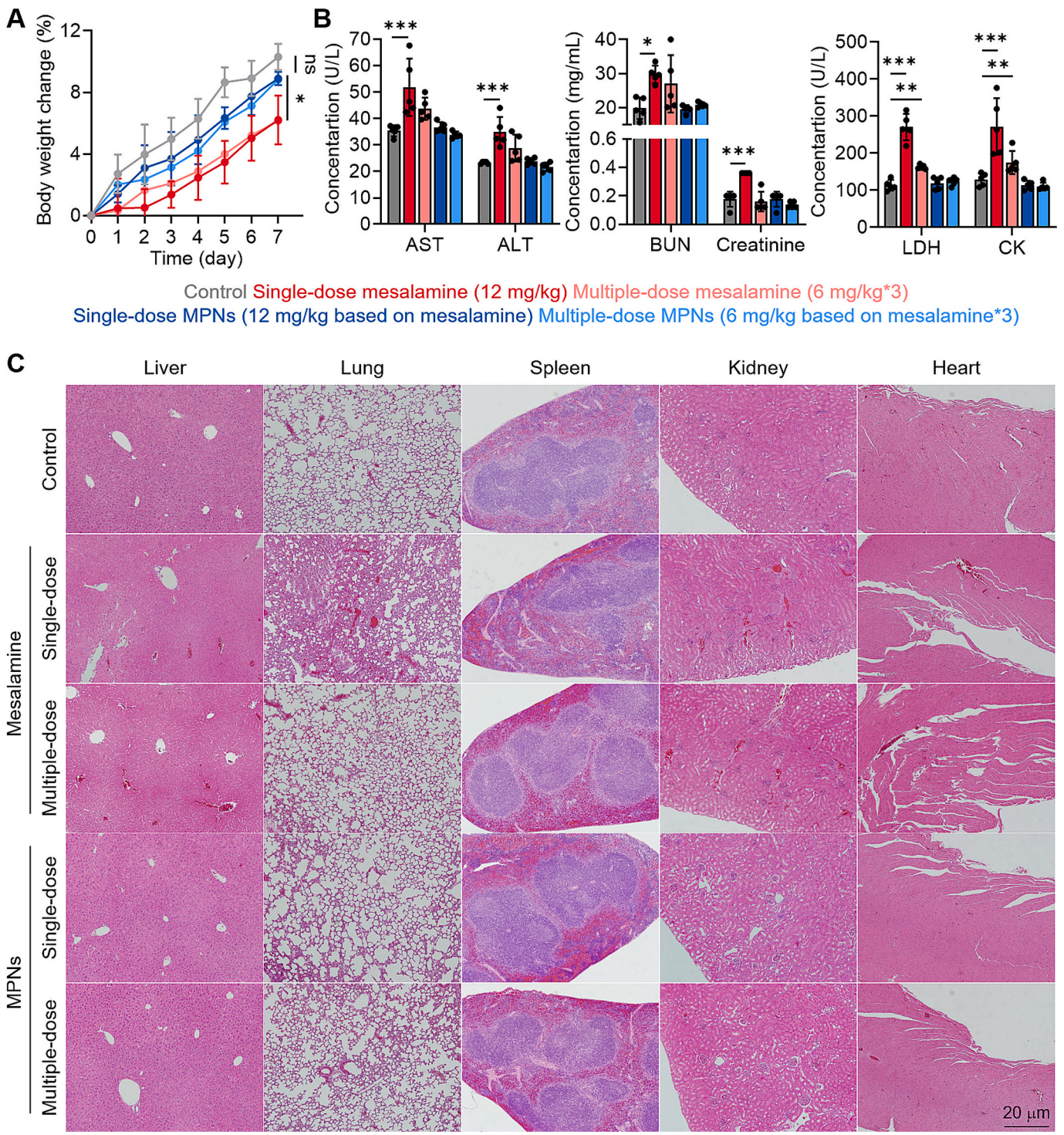


Fig. 5. Safety of MPN treatment. (A) Changes in body weight of healthy mice after treatment with a single or multiple dose of mesalamine or MPNs (n = 5). (B) Serem levels of hematological parameters related to hepatic, renal and cardiac functions (n = 5). (C) Major organs stained with H&E. $P^{ns} > 0.05$, $^{*}P < 0.05$, $^{**}P < 0.01$, $^{***}P < 0.001$; significance was determined by one-way ANOVA with Tukey's post hoc test.

3. Conclusion

The pathophysiology of acute kidney injury (AKI) involves a complex interplay of mechanisms, including inflammation, oxidative stress, mitochondrial dysfunction and vascular damage [34]. While these processes are essential for initiating renal repair, an imbalance during recovery can drive the progression to chronic kidney disease [35]. Among these mechanisms, inflammation plays a pivotal role in AKI progression. The activation of immune cells and the release of pro-inflammatory cytokines exacerbate tissue damage, impair repair processes and contribute to long-term fibrosis. Consequently, targeting inflammation represents a critical therapeutic strategy for improving outcomes in AKI [36,37].

The lack of effective organ-targeting treatments for kidney injury underscores a critical unmet need, as no drug from promising preclinical trials has advanced to routine clinical use. Drug repurposing involves re-

tasking existing medications for new clinical uses, offering advantages such as reduced cost and shorter development times [38]. Candidates are often identified through serendipity, data analysis or deeper understanding of disease mechanisms [39,40]. In the context of AKI, several repurposed drugs, including vasodilators like levosimendan and vitamin D, have been explored. Other examples include glucose-lowering drugs (SGLT2 inhibitors, GLP-1 agonists and metformin), xanthine oxidase inhibitors (allopurinol and febuxostat) and agents like baricitinib, abatacept, pentoxifylline and hydralazine [41].

This study explores repurposing mesalamine for the treatment of AKI. Mesalamine, a first-line anti-inflammatory drug for mild to moderate ulcerative colitis (UC), has also been used historically in Crohn's disease (CD) [42]. It remains a first-line therapy for over 50 % of patients with mild to moderate UC and may help reduce colon cancer risk in more severe cases. Despite its general safety, several instances of nephrotoxicity have been reported, though the underlying mechanisms remain unclear [12]. One hypothesis is that salicylates disrupt intrarenal prostaglandin synthesis and mitochondrial function, increasing oxidative stress.

The most common kidney-related adverse effect of mesalamine is interstitial nephritis. Animal studies have shown that even a single high dose can induce renal tubular and papillary necrosis [43]. Moreover, prolonged mesalamine use has been linked to chronic tubulointerstitial nephritis and tubular dysfunction, which may progress to chronic kidney disease [12]. Despite these renal complications, several animal studies suggest that mesalamine may have renoprotective effects due to its nitric oxide scavenging and antioxidative properties [10,44]. However, these promising mechanisms have not yet been translated into therapeutic applications for kidney diseases, as drug-induced renal complications remain a significant concern. The FDA and clinical guidelines advise caution when prescribing mesalamine or related compounds to patients with impaired renal function or a history of kidney disease. Regular monitoring of renal function is strongly recommended during mesalamine therapy [45,46]. In our IRI model, the inflamed kidneys are already highly susceptible to further injury due to compromised tubular integrity and increased oxidative stress. The systemic administration of free mesalamine may aggravate renal stress in this context, potentially explaining the enhanced TUNEL signal compared to PBS controls. These results underscore the need for controlled, site-specific delivery of mesalamine to minimize off-target toxicity, which our nanoassembly strategy addresses.

From this perspective, we proposed that developing a methodology to precisely control the pharmacokinetic and pharmacodynamic profiles of mesalamine for selective delivery to injured tubular cells could provide a potent and safe therapeutic option for AKI. Targeted delivery has traditionally been achieved using nanoparticulate systems, such as liposomes, polymeric nanoparticles and micelles [47]. However, since the maximum drug loading capacity is typically around 10 %, such carrier-based drug delivery system carry a risk of potential toxicity because patients are inevitably exposed to large amounts of carrier materials relative to the active ingredient [48,49]. In contrast, a prodrug designed in the present study is capable of self-assembling into nanoparticles through the intermolecular interactions, exhibiting in vivo behavior similar to that of conventional nanoparticles and ultimately enabling AKI biomarker-specific mesalamine delivery.

In the context of IRI–induced AKI, it is well established that tubular epithelial cells—particularly in the proximal tubules—are highly susceptible to injury and represent the primary site of pathological damage [50]. This susceptibility is largely due to their high metabolic demand and reliance on oxidative phosphorylation for active transport. Additionally, their location in the outer medulla, a region with relatively low oxygen tension, makes them particularly vulnerable to hypoxic injury. In our study, the accumulation of MPNs in the injured kidney was closely associated with areas showing tubular epithelial disruption and tight junction breakdown. This observation suggests that impaired tubular barrier integrity and altered tubular handling likely contribute to the renal retention and interstitial distribution of MPNs. Although the glomerular filtration barrier is generally impermeable to nanoparticles larger than 100 nm, we do not exclude the possibility of subtle glomerular filtration barrier alterations under AKI conditions. Our findings also showed that nanoparticles with a relatively larger size of 200 nm fail to accumulate in inflamed kidneys, highlighting the injured renal tissue-targeting mechanism of MPNs, which possess appropriate physical features.

Notably, selective accumulation of MPNs in the injured kidney significantly restored tight junction integrity, as evidenced by ZO-1 and occludin-1 levels that were nearly comparable to those in the Sham group. This was accompanied by a marked reduction in renal inflammatory cytokines, along with decreased infiltration of macrophages/monocytes and neutrophils. Interestingly, systemic inflammatory markers were also reduced by MPN treatment, whereas free mesalamine had no such effect. These results suggest that severe kidney inflammation in AKI contributes to systemic inflammation, and that targeted suppression of renal inflammation by MPNs can effectively mitigate this systemic response. This is further supported by previous studies demonstrating that AKI-induced systemic inflammation plays a critical role in the development of distant organ dysfunction and increased mortality [51], underscoring the potential clinical relevance of MPNs in preventing multiorgan complications associated with AKI.

In summary, this study offers a promising nanomedicine that maximizes anti-inflammatory effect of mesalamine in injured tubular cells, while minimizing its systemic toxicity and nephrotoxic risk. These findings support the potential repurposing of mesalamine, through a kidney-targeted prodrug approach, as a safe and effective therapeutic option for AKI.

4. Materials and methods

4.1. Preparation and physicochemical characterization

To prepare the mesalamine prodrug nanoassemblies (MPNs), the N-terminal acetylated Phe-Arg-Arg-Gly peptide (FRRG; 200 mg, 0.35 mmol, 1 eq; Peptron Co., Daejeon, Republic of Korea) was coupled with mesalamine (53.48 mg, 0.35 mmol, 1 eq; Tokyo Chemical Industry, Toshima, Tokyo, Japan) using carbonyldiimidazole (CDI; 67.5 mg, 0.42 mmol, 1.2 eq; Sigma-Aldrich, St. Louis, MO, USA) as an activating agent. After 30 min of reaction, the final product was purified and analyzed using an LC/MS system (Agilent 1200 Series HPLC system). The hydrodynamic size distribution and morphology were characterized using Zetasizer Nano ZS (Malvern Instruments, Worcestershire, UK) and transmission electron microscopy (TEM, CM-200, Philips, USA), respectively. To evaluate the serum stability, MPNs were incubated with mouse serum at 37 °C, followed by analysis of hydrodynamic size and polydispersity index (PDI) over 48 h. The cleavage behavior was assessed by HPLC after incubation of MPNs with cathepsin B (953CY, R&D systems, MN, USA), cathepsin L (952-CY, R&D systems), cathepsin E (1294-AS, R&D systems), cathepsin D (1014-AS, R&D systems), caspase-3 (707-C3/CF, R&D systems) or MMP-9 (911-MP, R&D systems).

The cytotoxicity of mesalamine or MPNs was assessed in the normal human proximal tubule cell line HK-2 (American Type Culture Collection, Manassas, VA, USA). Briefly, 5×10^3 HK-2 cells were seeded into 96-well cell culture plates and treated with different concentrations ranging from 0.01 mM to 25 mM based on mesalamine content for 24 h. Finally, the cell viability was measured using a UV/Vis microplate reader after incubation with 10 % Cell Counting Kit-8 (CCK-8, Dojindo, Tabaru, Japan).

For fluorescence imaging, Cy5.5-labeled MPNs were prepared as follows: NH_2-FRRG-COOH peptide (Peptron Co.;178.26 mg, 0.39 mmol), Cy5.5 NHS ester (Lumiprobe, Wan Chai, Hong Kong; 150 mg, 0.195 mmol) and N, N diisopropylethylamine (DIPEA, Sigma Aldrich; 30.18 mg, 0.234 mmol) were mixed in anhydrous dimethylformamide

(DMF). After 3 h of reaction, Cy5.5-FRRG-COOH was purified using Sep-Pak C18 cartridges (Waters, Massachusetts, USA) and subsequently coupled with mesalamine following the same method described above. Cy5.5-conjugated mesalamine prodrug and unmodified mesalamine prodrug were evenly mixed in saline at a 1:99 wt%, resulting in Cy5.5-labeled nanoassemblies.

4.2. Anti-inflammatory effect by the inhibition of MAPK signaling pathway

To analyze changes in cathepsin B expression under injured conditions, HK-2 cells were treated with 500 μM H_2O_2. After 4 h of incubation, the cells were washed twice with DPBS and dispersed in lysis buffer (1 % sodium deoxycholate, 0.1 % SDS, 1 % NP-40, 25 mM Tris-HCl, 150 mM NaCl and 1 % protease inhibitor). The proteins were quantified using a BCA assay kit (23,221, Thermo Fisher Scientific) and were then mixed with sodium dodecyl sulfate loading buffer. After boiling for 5 min, the protein samples were separated on a 10 % SDS polyacrylamide gel and subsequently transferred onto a nitrocellulose membrane. The membranes were blocked with TBS-T buffer containing 3 % BSA for 1 h at room temperature, followed by an overnight incubation at 4 °C with antibodies against cathepsin B (sc-365,558, Santa Cruz Biotechnology, Dallas, Texas, USA) or β-actin (ab8227, Abcam, Cambridge, UK). The membranes were further incubated with anti-mouse or anti-rabbit immunoglobulins-horseradish peroxidase (HRP) antibodies for 1 h. HRP signal intensities on membranes were detected using an enhanced chemiluminescence system.

To evaluate the MAPK-inhibitory effects, HK-2 cells were seeded into 6-well culture plates at a density of 5×10^5 cells per well. After 24 h incubation, the cells were treated with either mesalamine or MPNs in the presence of 500 uM H_2O_2 for 4 h. Following treatment, western blot analyses were performed using the same protocol described above to assess MAPK signaling pathway activation by measuring the expression levels of KIM-1, phosphorylated JNK and phosphorylated p38.

4.3. Human samples

We performed a retrospective review of medical records from February 2013 to November 2023, comparing two groups: patients with AKI, including eight individuals with histologically confirmed acute tubular necrosis (ATN) or acute tubulointerstitial nephritis (ATIN) without evidence of chronic lesions and ten patients who underwent kidney biopsy or partial nephrectomy due to suspected renal cell carcinoma but showed normal histology or only mild glomerular alterations. The study was approved by our institutional review board and complied with the ethical standards of the Declaration of Helsinki (IRB No 2025AN0064).

4.4. Animal study

All experiments involving animals were conducted in accordance with relevant laws and institutional guidelines of the Institutional Animal Care and Use Committee (IACUC, approved number: 2023–013) at the KIST. The C57BL/6 mice were purchased from NaraBio (Republic of Korea) and bred under pathogen-free conditions at KIST. All mice were housed under a 12/12-h light-dark cycle with free access to water and food, except for fasting on the day of bilateral renal surgery. For the surgical procedure, the mice were anesthetized with a mixture of Zoletil and Rompun. All animal experiments were conducted using six-week-old male C57BL/6 mice because female C57BL/6 mice are resistant to AKI [52].

4.5. Biodistribution

The renal accumulation of MPNs was compared between healthy mice and AKI mice. AKI mice were prepared in C57BL/6 mice by clamping the renal pedicles for 30 min to induce ischemia, followed by reperfusion (IRI). To evaluate the in vivo biodistribution in both mice models, NIRF imaging was performed using the Lumina Series III system (PerkinElmer, USA) after intravenous injection of Cy5.5-labeled MPNs. As a control, HA nanoparticles—prepared by modifying hyaluronic acid (HA-101, Creative PEGWorks) with hydrophobic Cy5.5 amine (470C0, Lumiprobe) via amide condensation—were intravenously administered. Fluorescence intensity in NIRF images was quantified using LivingImage software (PerkinElmer, USA). Ex vivo NIRF imaging was performed on major organs, including the liver, lungs, spleen, kidneys and heart, which were collected 6, 12, 24 or 48 h after treatment from the mice. Subsequently, kidney tissues were sectioned coronally and sagittally at a thickness of 20 μm and stained with a 4′,6-diamidino-2-phenylindole (DAPI, Invitrogen, USA). The presence of MPNs within the kidney tissues was observed using confocal laser scanning microscopy (Leica, Germany).

To assess the PK profiles, MPNs were administered intravenously to AKI mice at a dose corresponding to 6 mg/kg of mesalamine. Blood samples were collected at the indicated time points, centrifuged for 20 min at 2200 rpm, and the resulting serum was treated with acetonitrile (1:3, *v*/v) for protein precipitation. Fluorescence intensities in the supernatants were then quantified using a Lumina Series III (PerkinElmer, USA). For PD analysis, major organs (liver, lung, kidney and heart) and injured kidney tissue were collected and subjected to protein quantification. Cathepsin B expression in each sample was evaluated by western blot as described above. Equal amounts of protein lysates from each organ were incubated with MPNs for 48 h, followed by HPLC analysis.

4.6. Therapeutic efficacy

To evaluate therapeutic efficacy, AKI mice were intravenously administrated PBS, mesalamine (6 mg/kg) or MPNs (1, 3 or 6 mg/kg based on mesalamine content) 1 h after IRI injury. Following 24 h of treatment, whole blood was collected via the inferior vena cava. The blood samples were centrifuged to obtain serum, which was then analyzed for kidney injury markers, including blood urea nitrogen (BUN) and creatinine. The supernatants from homogenized kidney tissues were analyzed for inflammatory cytokines such as TNF-α (43,907, BioLegened, CA, USA), IL-1β (MLB00C, R&D systems), IL-6 (M6000B, R&D systems) and IL-10 (DY217B, R&D systems) using ELISA assays. Additionally, portion of kidney tissues were subjected to immunohistochemical staining with PAS, F4/80 (MCA497G, Serotec) antibody, Ly6G (11–9668, eBioscience) antibody or terminal deoxynucleotidyl transferase dUTP nick-end labeling (TUNEL) to assess tissue damage and inflammation. Tubular injury, including necrotic tubules, formation of tubular casts and loss of brush borders, was quantified using a scoring system from 0 to 4, with the average score calculated. All evaluations of the slides were performed in a blinded manner. To quantify the staining, 5–6 high-power fields were randomly selected from each slide. Positive cell areas were measured and compared between groups using Fiji ImageJ software (NIH, USA).

4.7. Evaluation of systemic inflammation

The tight junction disruption in the kidneys was evaluated by analyzing the levels of occludin-1 and ZO-1. Following the previously described protocol [26,53], the kidney tissues collected from healthy or AKI mice were stained using a mouse anti-mouse Alexa Fluor 488-conjugated occludin-1 antibody (TFS-331588, Invitrogen, USA) and a rabbit anti-mouse Alexa Fluor 647-conjugated ZO-1 antibody (98225S, Cell Signaling, USA). The levels of TNF-α, IFN-γ, IL-1β, IL-6 and IL-10 in seum samples were analyzed via ELISA assays to evaluate systemic inflammatory responses. Additionally, the following hematological parameters from AKI mice treated with PBS, mesalamine or MPNs were analyzed: aspartate aminotransferase (AST), alanine transaminase (ALT), lactate dehydrogenase (LDH) and creatinine kinase (CK) in the serum; and

white blood cell (WBC), neutrophil (NEU), lymphocyte (LYM), monocyte (MONO) and platelet (PLT) in the whole blood. Major organs, including the liver, lungs, spleen, kidneys and heart, colledted from the mice were stained with H&E and subsequently examined using microscopy (BX 51, Olympus, USA).

4.8. Biocompatibility

To assess in vivo safety, healthy 6-week-old male C57BL/6 mice were intravenously administered mesalamine or MPNs, either as a high/single dose (12 mg/kg based on mesalamine content) or as multiple doses (6 mg/kg based on mesalamine content) over three consecutive days. Body weights were measured daily. On day 7, blood samples and major organs were collected for further analysis: AST, ALT, BUN, creatinine, LDH and CK in the serum; and structural abnormalities in the major organs stained with H&E.

4.9. Statistical analysis

Statistical significance between the two groups was analyzed using the Student's *t*-test. In the case of more than two groups, one-way analysis of variance (ANOVA) was used, and multiple comparisons were performed using the Tukey-Kramer post-hoc test. Survival results were plotted using Kaplan−Meier curves and analyzed using the log-rank test. All results are presented as mean ± SD, and *P* values of $>0.05^{ns}$, <0.05*, <0.01** and <0.001*** were considered statistically significant.

CRediT authorship contribution statement

Byeongmin Park: Writing – original draft, Methodology, Investigation, Formal analysis, Data curation. **Daeho Park:** Writing – original draft, Methodology, Investigation, Formal analysis. **Hochung Jang:** Writing – original draft, Methodology, Investigation, Formal analysis. **Yoon Sook Ko:** Methodology, Investigation. **Hee Young Lee:** Investigation. **Young Eun Choi:** Investigation. **Jiwoong Choi:** Investigation. **Se Won Oh:** Investigation. **Sang-Kyung Jo:** Methodology. **Sun Hwa Kim:** Methodology. **Yongju Kim:** Methodology. **Sangmin Lee:** Methodology. **Kwangmeyung Kim:** Methodology. **Myung-Gyu Kim:** Writing – original draft, Supervision, Resources, Project administration. **Yoosoo Yang:** Writing – original draft, Supervision, Resources, Project administration, Funding acquisition. **Man Kyu Shim:** Writing – original draft, Supervision, Resources, Project administration, Methodology, Funding acquisition, Conceptualization.

Declaration of competing interest

The authors declare no competing financial interests.

Acknowledgments

This work was supported by grants from the National Research Foundation (NRF) of Korea, funded by the Ministry of Science (RS-2025-02219039, RS-2021-NR061836, 2022R1A2C2006861, RS-2024-00452747, RS-2021-NR061836 and RS-2024-00463774) and the Intramural Research Program of KIST.

Appendix A. Supplementary data

Supplementary data to this article can be found online at https://doi.org/10.1016/j.jconrel.2025.114041.

Data availability

The underlying data from the manuscript are available from the corresponding author upon request. All the uncropped western blot source data are presented in Supplementary materials file. All the uncropped western blot source data are presented in Fig. S16.

References

[1] A.J. Lewington, J. Cerdá, R.L. Mehta, Raising awareness of acute kidney injury: a global perspective of a silent killer, Kidney Int. 84 (2013) 457–467.
[2] M.E. Thomas, C. Blaine, A. Dawnay, M.A. Devonald, S. Ftouh, C. Laing, S. Latchem, A. Lewington, D.V. Milford, M. Ostermann, The definition of acute kidney injury and its use in practice, Kidney Int. 87 (2015) 62–73.
[3] T.A. Ikizler, C.R. Parikh, J. Himmelfarb, V.M. Chinchilli, K.D. Liu, S.G. Coca, A. X. Garg, C.-Y. Hsu, E.D. Siew, M.M. Wurfel, A prospective cohort study of acute kidney injury and kidney outcomes, cardiovascular events, and death, Kidney Int. 99 (2021) 456–465.
[4] J.A. Kellum, P. Romagnani, G. Ashuntantang, C. Ronco, A. Zarbock, H.-J. Anders, Acute kidney injury, Nat. Rev. Dis. Primers 7 (2021) 1–17.
[5] M.T. James, M. Bhatt, N. Pannu, M. Tonelli, Long-term outcomes of acute kidney injury and strategies for improved care, Nat. Rev. Nephrol. 16 (2020) 193–205.
[6] C.Y. Chionh, S.S. Soni, F.O. Finkelstein, C. Ronco, D.N. Cruz, Use of peritoneal dialysis in AKI: a systematic review, Clin. J. Am. Soc. Nephrol. 8 (2013) 1649–1660.
[7] S. Pushpakom, F. Iorio, P.A. Eyers, K.J. Escott, S. Hopper, A. Wells, A. Doig, T. Guilliams, J. Latimer, C. McNamee, Drug repurposing: progress, challenges and recommendations, Nat. Rev. Drug Discov. 18 (2019) 41–58.
[8] P. Zhan, B. Yu, L. Ouyang, Drug repurposing: an effective strategy to accelerate contemporary drug discovery, Drug Discov. Today 27 (2022) 1785.
[9] G.C. Kaiser, F. Yan, D.B. Polk, Mesalamine blocks tumor necrosis factor growth inhibition and nuclear factor κB activation in mouse colonocytes, Gastroenterology 116 (1999) 602–609.
[10] M. Kennedy, L. Wilson, C. Szabo, A.L. Salzman, 5-aminosalicylic acid inhibits iNOS transcription in human intestinal epithelial cells, Int. J. Mol. Med. 4 (1999) 437–480.
[11] P.J. Margetts, D.N. Churchill, I. Alexopoulou, Interstitial nephritis in patients with inflammatory bowel disease treated with mesalamine, J. Clin. Gastroenterol. 32 (2001) 176–178.
[12] A. Adiga, D.S. Goldfarb, The association of mesalamine with kidney disease, Adv. Chronic Kidney Dis. 27 (2020) 72–76.
[13] A.I. Qureshi, R.D. Cohen, Mesalamine delivery systems: do they really make much difference? Adv. Drug Deliv. Rev. 57 (2005) 281–302.
[14] K. Fukunaga, Y. Ohda, T. Inoue, T. Kono, H. Miwa, T. Matsumoto, Toxic epidermal necrosis associated with mesalamine in a patient with ulcerative colitis, Inflamm. Bowel Dis. 13 (2007) 1055–1056.
[15] T. Putnam, E. Turse, K. Kadkhodayan, 2083 Mesalamine-induced myocarditis, Am. J. Gastroenterol. 114 (2019) (2025) S1161–S1162.
[16] M.J. Chung, J.H. Lee, K.R. Moon, Mesalizine-induced acute pancreatitis and interstitial pneumonitis in a patient with ulcerative colitis, Pediatr. Gastroenterol. Hepatol. Nutr. 18 (2015) 286–291.
[17] Q. Cheng, A. Hao, P. Xing, Engineering π-conjugation of phenylalanine derivatives for controllable chiral folding and self-assemblies, ACS Nano 18 (2024) 5766–5777.
[18] Y. Moon, H. Cho, J. Kim, S. Song, J. Yeon Park, J. Young Min, E. Hee Han, Y. Kim, J.K. Seong, M. Kyu Shim, Self-assembled peptide-derived proteolysis-targeting chimera (PROTAC) Nanoparticles for tumor-targeted and durable PD-L1 degradation in Cancer immunotherapy, Angew. Chem. Int. Ed. 64 (2025) e202414146.
[19] M.K. Shim, J. Park, H.Y. Yoon, S. Lee, W. Um, J.-H. Kim, S.-W. Kang, J.-W. Seo, S.-W. Hyun, J.H. Park, Carrier-free nanoparticles of cathepsin B-cleavable peptide-conjugated doxorubicin prodrug for cancer targeting therapy, J. Control. Release 294 (2019) 376–389.
[20] M.K. Shim, Y. Moon, S. Yang, J. Kim, H. Cho, S. Lim, H.Y. Yoon, J.-K. Seong, K. Kim, Cancer-specific drug-drug nanoparticles of pro-apoptotic and cathepsin B-cleavable peptide-conjugated doxorubicin for drug-resistant cancer therapy, Biomaterials 261 (2020) 120347.
[21] Y. Moon, M.K. Shim, J. Choi, S. Yang, J. Kim, W.S. Yun, H. Cho, J.Y. Park, Y. Kim, J.-K. Seong, Anti-PD-L1 peptide-conjugated prodrug nanoparticles for targeted cancer immunotherapy combining PD-L1 blockade with immunogenic cell death, Theranostics 12 (2022) 1999.
[22] M.K. Shim, H.Y. Yoon, J.H. Ryu, H. Koo, S. Lee, J.H. Park, J.-H. Kim, S. Lee, M. G. Pomper, I.C. Kwon, K. Kim, Cathepsin B-specific metabolic precursor for in vivo tumor-specific fluorescence imaging, Angew. Chem. Int. Ed. 55 (2016) 14698–14703.
[23] J. Choi, B. Park, J.Y. Park, D. Shin, S. Lee, H.Y. Yoon, K. Kim, S.H. Kim, Y. Kim, Y. Yang, Light-triggered PROTAC nanoassemblies for photodynamic IDO proteolysis in cancer immunotherapy, Adv. Mater. 36 (2024) 2405475.
[24] N. Shim, S.I. Jeon, S. Yang, J.Y. Park, M. Jo, J. Kim, J. Choi, W.S. Yun, J. Kim, Y. Lee, Comparative study of cathepsin B-cleavable linkers for the optimal design of cathepsin B-specific doxorubicin prodrug nanoparticles for targeted cancer therapy, Biomaterials 289 (2022) 121806.
[25] J. Choi, M.K. Shim, S. Yang, H.S. Hwang, H. Cho, J. Kim, W.S. Yun, Y. Moon, J. Kim, H.Y. Yoon, Visible-light-triggered prodrug nanoparticles combine chemotherapy and photodynamic therapy to potentiate checkpoint blockade cancer immunotherapy, ACS Nano 15 (2021) 12086–12098.
[26] B. Park, G. Han, D.Y. Jin, K.C. Gil, D. Shin, J. Lee, J.Y. Park, H. Jang, D. Park, S. Lee, K. Kim, Y. Yang, Y. Kim, J.-S. Kim, S.H. Kim, M.K. Shim, Mucoadhesive

Mesalamine prodrug Nanoassemblies to target intestinal macrophages for the treatment of inflammatory bowel disease, ACS Nano 18 (2024) 16297–16311.
[27] J. Kim, M.K. Shim, S. Yang, Y. Moon, S. Song, J. Choi, J. Kim, K. Kim, Combination of cancer-specific prodrug nanoparticle with Bcl-2 inhibitor to overcome acquired drug resistance, J. Control. Release 330 (2021) 920–932.
[28] S. Yang, M.K. Shim, W.J. Kim, J. Choi, G.-H. Nam, J. Kim, J. Kim, Y. Moon, H. Y. Kim, J. Park, Cancer-activated doxorubicin prodrug nanoparticles induce preferential immune response with minimal doxorubicin-related toxicity, Biomaterials 272 (2021) 120791.
[29] S. Kishi, H. Nagasu, K. Kidokoro, N. Kashihara, Oxidative stress and the role of redox signalling in chronic kidney disease, Nat. Rev. Nephrol. 20 (2024) 101–119.
[30] S. Behzadi, V. Serpooshan, W. Tao, M.A. Hamaly, M.Y. Alkawareek, E.C. Dreaden, D. Brown, A.M. Alkilany, O.C. Farokhzad, M. Mahmoudi, Cellular uptake of nanoparticles: journey inside the cell, Chem. Soc. Rev. 46 (2017) 4218–4244.
[31] B. Du, M. Yu, J. Zheng, Transport and interactions of nanoparticles in the kidneys, Nat. Rev. Mater. 3 (2018) 358–374.
[32] Y.-N. Zhang, W. Poon, A.J. Tavares, I.D. McGilvray, W.C. Chan, Nanoparticle–liver interactions: cellular uptake and hepatobiliary elimination, J. Control. Release 240 (2016) 332–348.
[33] N.C. Teoh, G.C. Farrell, Hepatic ischemia reperfusion injury: pathogenic mechanisms and basis for hepatoprotection, J. Gastroenterol. Hepatol. 18 (2003) 891–902.
[34] A. Agarwal, Z. Dong, R. Harris, P. Murray, S.M. Parikh, M.H. Rosner, J.A. Kellum, C. Ronco, A.D.Q.I.X.W. Group, Cellular and molecular mechanisms of AKI, J. Am. Soc. Nephrol. 27 (2016) 1288–1299.
[35] S.G. Coca, S. Singanamala, C.R. Parikh, Chronic kidney disease after acute kidney injury: a systematic review and meta-analysis, Kidney Int. 81 (2012) 442–448.
[36] H. Rabb, M.D. Griffin, D.B. McKay, S. Swaminathan, P. Pickkers, M.H. Rosner, J. A. Kellum, C. Ronco, Inflammation in AKI: current understanding, key questions, and knowledge gaps, J. Am. Soc. Nephrol. 27 (2016) 371–379.
[37] Y. Sato, M. Yanagita, Immune cells and inflammation in AKI to CKD progression, Am. J. Physiol.-Renal Physiol. 315 (2018) F1501–F1512.
[38] C. Harrison, Signatures for drug repositioning, Nat. Rev. Genet. 12 (2011) 669.
[39] R. Liu, L. Wei, P. Zhang, A deep learning framework for drug repurposing via emulating clinical trials on real-world patient data, Nat. Mach. Intell. 3 (2021) 68–75.
[40] Z.-Y. Wang, H.-Y. Zhang, Rational drug repositioning by medical genetics, Nat. Biotechnol. 31 (2013) 1080–1082.
[41] U. Panchapakesan, C. Pollock, Drug repurposing in kidney disease, Kidney Int. 94 (2018) 40–48.
[42] R. Chibbar, A.C. Moss, Mesalamine in the initial therapy of ulcerative colitis, Gastroenterol. Clin. 49 (2020) 689–704.
[43] I. Calder, C. Funder, C. Green, K.N. Ham, J. Tange, Nephrotoxic lesions from 5-aminosalicylic acid, Br. Med. J. 1 (1972) 152–154.
[44] S. Banaei, The effect of 5-aminosalicylic acid on renal ischemia-reperfusion injury in rats, Indian J. Pharm. 48 (2016) 196–199.
[45] A. Kornbluth, D.B. Sachar, P.P.C.o.t.A.C.o., Gastroenterology, ulcerative colitis practice guidelines in adults: American college of gastroenterology, practice parameters committee, Am. J. Gastroenterol. 105 (2010) 501–523.
[46] C. Mowat, A. Cole, A. Windsor, T. Ahmad, I. Arnott, R. Driscoll, S. Mitton, T. Orchard, M. Rutter, L. Younge, Guidelines for the management of inflammatory bowel disease in adults, Gut 60 (2011) 571–607.
[47] J.D. Byrne, T. Betancourt, L. Brannon-Peppas, Active targeting schemes for nanoparticle systems in cancer therapeutics, Adv. Drug Deliv. Rev. 60 (2008) 1615–1626.
[48] M. Tarannum, J.L. Vivero-Escoto, Nanoparticle-based therapeutic strategies targeting major clinical challenges in pancreatic cancer treatment, Adv. Drug Deliv. Rev. 187 (2022) 114357.
[49] M. Kyu Shim, S. Yang, I.-C. Sun, K. Kim, Tumor-activated carrier-free prodrug nanoparticles for targeted cancer immunotherapy: preclinical evidence for safe and effective drug delivery, Adv. Drug Deliv. Rev. 183 (2022) 114177.
[50] J.V. Bonventre, L. Yang, Cellular pathophysiology of ischemic acute kidney injury, J. Clin. Invest. 121 (2011) 4210–4221.
[51] R. Matsuura, K. Doi, H. Rabb, Acute kidney injury and distant organ dysfunction–network system analysis, Kidney Int. 103 (2023) 1041–1055.
[52] K.P. Kang, J.E. Lee, A.S. Lee, Y.J. Jung, D. Kim, S. Lee, H.P. Hwang, W. Kim, S. K. Park, Effect of gender differences on the regulation of renal ischemia-reperfusion-induced inflammation in mice, Mol. Med. Rep. 9 (2014) 2061–2068.
[53] B. Park, E.H. Kim, H. Jang, Y. Kim, Y. Ryu, J. Choi, D. Shin, M.C. Lee, Y. Yang, K. Kim, S. Lee, S.H. Kim, M.K. Shim, Drug repositioning of mesalamine via supramolecular nanoassembly for the treatment of drug-induced acute liver failure, Theranostics 15 (2025) 1122–1134.